Contents lists available at SciOpen

Food Science and Human Wellness

journal homepage: https://www.sciopen.com/journal/2097-0765

China Food Publishing Co.

Rational protein engineering of thermostable heparinase I from *Bacteroides thetaiotaomicron* for highly efficient heparin degradation

Chuan Zhang[a,b], Ruohan Zhao[a,b], Leilei Yu[a,b], Qixiao Zhai[a,b], Jianxin Zhao[a,b], Hao Zhang[a,b], Xuegang Luo[c,*], Fengwei Tian[a,b,*], Wei Chen[a,b,d]

[a] *State Key Laboratory of Food Science and Technology, Jiangnan University, Wuxi 214122, China*
[b] *School of Food Science and Technology, Jiangnan University, Wuxi 214122, China*
[c] *Key Laboratory of Industrial Fermentation Microbiology of the Ministry of Education, Tianjin Key Lab of Industrial Microbiology, College of Biotechnology, Tianjin University of Science and Technology, Tianjin 300457, China*
[d] *National Engineering Research Center for Functional Food, Jiangnan University, Wuxi 214122, China*

ARTICLE INFO

Article history:
Received 8 February 2023
Received in revised form 22 March 2023
Accepted 24 May 2023

Keywords:
Heparin
Bacteroides thetaiotaomicron
Heparinase I
Rational protein engineering
Thermostability

ABSTRACT

Heparin, a glycosaminoglycan, is a stable source of carbon that supports the growth of microorganisms in the human intestine. It is also a commonly used anticoagulant drug in clinical practice, with significant therapeutic effects. Low molecular weight heparin (LMWH) is a highly active low molecular weight fragment obtained *via* enzymatic reaction or the chemical degradation of heparin. LMWH has been applied globally in the prevention and treatment of venous thromboembolism in thrombosis patients. Simultaneously, as a potential prebiotic, because of its low molecular weight, LMWH can be well degraded by the gut microbiota to maintain intestinal balance. Enzymatic heparin degradation has recently emerged as a viable disposal method for LMWH preparation; however, only very few benchmark enzymes have been thoroughly described and subjected to protein engineering to improve their properties over the past few years. The commercialization of enzymes will require the development of robustly engineered enzymes that meet the demands of industrial processes. Herein, we report a rational protein engineering strategy that includes molecular dynamic simulations of flexible amino acid mutations and disulfide bond screening. Several *Bacteroides thetaiotaomicron* heparanase I (Bt-HepI) mutants were obtained and screened for high thermal stability. We obtained the Bt-HepI$^{D204C/K208C/H189W/Q198R}$ variant, which features a stabilized protein surface structure, with a 1.3-fold increase in catalytic constant/michaelis-menten constant (k_{cat}/K_m), a 2.44-fold increase in thermal stability at 50 °C, and a 1.8-fold decrease in the average molecular weight of LMWH produced at 40 °C compared with that seen with Bt-HepI^{WT}. Our study establishes a strategy to engineer thermostable HepI to underpin its industrial applications.

1. Introduction

Heparin, a member of the glycosaminoglycan family, is an acidic mucopolysaccharide composed of repeating units of iduronic and glucuronic acid disaccharides[1]. Heparin can specifically bind to antithrombin to exert its anticoagulant function[2-5]. Commercial heparin is primarily extracted from the mucosa of the bovine lung and porcine small intestine currently[6]. The extracted heparin has a complex structure and several crucial biological functions and is generally used clinically for the treatment of thrombosis, cardiovascular disease, and other diseases[7-8]. It also serves as a stable carbon source for the host intestine, can effectively regulate the structure of intestinal flora, and has potential prebiotic functions[9].

* Corresponding authors.
E-mail address: luoxuegang@hotmail.com (X.G. Luo);
fwtian@jiangnan.edu.cn (F.W. Tian)

Peer review under responsibility of Beijing Academy of Food Sciences.

SciOpen Publishing services by Tsinghua University Press

http://doi.org/10.26599/FSHW.2024.9250134

Low molecular weight heparin (LMWH) is a small heparin fraction produced by heparin cleavage, which has a reduced ability to bind proteins or cells but significantly increased anticoagulant activity. LMWH has various advantages over heparin, such as higher utilization, longer half-life, and fewer side effects[10-11]. In addition, the low molecular weight of LMWH allows, it to be better degraded by gut microbes, which helps maintain intestinal homeostasis. Therefore, the methods for preparing LMWH are important. Physical, chemical, biological, and synthetic approaches are currently being used to prepare LMWH. In recent years, biological enzymatic catalysis has emerged as a potentially attractive alternative to more traditionally cleaved heparin strategies, because of its advantages, including mild conditions, high selectivity, and low pollution.

Heparinase I (HepI) is a class of polysaccharide cleaving enzymes capable of cleaving heparin to prepare LMWH. HepI is found in a wide range of sources, primarily in *Flavobacterium heparinum* and *Bacteroides*[12]. Recent studies have shown that human gut microorganisms can effectively degrade heparin[13-14], with *Bacteroides* being the major contributor[15]. Other studies have reported the isolation of highly active HepI from *Bacteroides eggerthii* and *Bacteroides cellulosilyticus*[16-17]. These studies focused only on the activity of HepI, ignoring its thermal stability. The crystal structure of HepI from *Bacteroides thetaiotaomicron* (Bt-HepI) has been widely studied, and its specific degradation mechanism has been resolved[18]. The unique catalytic properties of Bt-HepI make it an attractive candidate as a biocatalyst for LMWH preparation. Unfortunately, the wild-type enzyme has low thermostability[19], suggesting that bio-transformations must be performed at ambient temperatures far below the temperature. This compromises heparin deconstruction rates and decreases the storage time of the enzyme. To address these limitations, improvements in HepI stability have been achieved using a variety of rational engineering approaches[20]. One study documented the improved thermal stability of HepI using the fused maltose binding protein (MBP). The authors also reported that stability was improved by mutating the C297 site, which was used to inhibit dimerization[19].

Thus far, there have been few reports on the thermal stability of HepI. In contrast, experimental optimization of enzymes using rational protein engineering typically offers a more comprehensive approach to the enzyme engineering[21-24], and molecular dynamics simulations (MDs) have demonstrated the flexible region of the enzyme. The root mean square deviation (RMSD) is an important parameter that reflects the flexibility of the protein residues[25]. The higher the root mean square fluctuation (RMSF) value of the residue higher the degree of freedom. The flexible region consists of residues with high RMSF values. Disulfide bonds play a crucial role in protein folding and stability, stabilizing the structure and regulating the activity of proteins[26-29]. Structure-based design methods used to form disulfide bonds in proteins to improve protein stability have achieved considerable success in biopharmaceutical and industrial applications[30]. Here, based on the reported crystal structure of Bt-HepI, we developed a rational protein engineering strategy to obtain Bt-HepI mutants with remarkably enhanced thermal stability and improved heparin degradation ability. The findings should help expand the applications of Bt-HepI in human pharmaceutical and food industries.

2. Materials and methods

2.1 Materials

Escherichia coli DH5α and BL21 (DE3) were obtained from our laboratory culture collection. The gene encoding Bt-HepI was codon optimized and commercially synthesized by GENEWIZ Co., Ltd. (Suzhou, China), and then cloned into the *BamH* I and *Xho* I sites of the pE-SUMO vector. Heparin sodium salt (185 U/mg) was purchased from Sangong Shanghai (China). 2× Phanta Max Master Mix DNA Polymerase was purchased from Vazyme Biotechnology Co., Ltd. (Nanjing, China). His GraviTrap TALON was purchased from GE Healthcare (Little Chalfont, UK). All other reagents were purchased from Sinopharm Group Chemical Reagent Co., Ltd. (Shanghai, China).

2.2 MDs and flexible virtual mutation screening

The 3-dimensional structure of Bt-HepI was obtained from the Protein Data Bank (PDB ID: 3ikw). The three-dimensional structures of mutants were determined using PyMOL software simulation according to the Bt-HepI structure. MDs of Bt-HepI were performed using Amber16 software under 333 K and 100 ns conditions. To fix the protein with a force of 3 000 kcal/(mol·Å2), the solution was first optimized using the steepest descent method with 2 000 steps and the conjugate gradient method with 2 000 steps. To optimize the side chains, atoms in the backbone structure of the protein were fixed at a force of 500 kcal/(mol · Å2). Overall optimization was performed without any restrictions on the entire system. In an MDs a heating stage was used to steadily increase the temperature over 50 ps from 0 K to 300 K. Next, a constant number, pressure, and temperature simulation was performed for 100 ps at 300 K. Constant temperature and volume simulations were performed for 50 ns, and the bonds involving hydrogen atoms were optimized using SHAKE. Amber16 was used to construct an electronic library of thermostable HepI mutants based on the RMSF and *D*-stability values.

2.3 Disulfide bond screening

Disulfide bond scanning of the Bt-HepI (3ikw) was performed to construct an electronic library of mutations using the disulfide scan module of Amber16 MOE. Unary quadratic optimization in LowMode was used to scan for mutations. LowModeMD was used to search the conformational space of the mutants. The LowModeMD search method, with an MD run of approximately 1 ps at a constant temperature, was followed by whole-atom energy minimization to generate mutant conformations. The results were saved in the output database when the conformations results satisfied the requirements of the energetic and geometric criteria. To accelerate MDs, atoms over 4.5 Å were labeled as inert, and the number of iterations was limited to 50. The conformation of each complex mutation was limited to 5. Finally, the mutant stabilities were determined. Based on the *D*-stability values of the HepI mutants, *D*-stability < −5 kcal/mol was used as the screening criterion to construct an electronic library. The Pymol software program was used to screen for unreasonable mutants in electronic libraries.

2.4 Protein preparation

The Bt-HepI gene was amplified through polymerase chain reaction (PCR) using a synthesized gene with codon optimization for expression in *E. coli* as a template. The nucleotide sequence corresponding to the signal peptide was removed from the synthetic DNA. The amplified product was subcloned into the pE-SUMO expression vector, and the pE-SUMO-Bt-HepI plasmid was transformed into *E. coli* BL21 (DE3) cells for growth at 37 ℃ in fresh Luria-Bertani medium containing 50 μg/mL kanamycin. After inducing protein expression by adding 0.6 mmol/L isopropyl *β-D*-1-thiogalactopyranoside, the culture was further incubated for 12 h at 25 ℃. The cells were harvested by centrifugation at 8 000 × *g* for 5 min at room temperature. The cell pellet was resuspended in Tris-HCl buffer (20 mmol/L Tris, 200 mmol/L NaCl, and 5 mmol/L $CaCl_2$ at pH 7.4) and disrupted by repeated ultrasonication (300 W for 3 s, stop for 4 s) for 10 min. The cell debris was removed by centrifugation at 12 000 × *g* for 30 min at 4 ℃. The supernatant was applied to a Ni-Trap metal chelate column (GE Healthcare). The column was washed with 10 mL of buffer (50 mmol/L Tris, 300 mmol/L NaCl, 5 mmol/L $CaCl_2$, and 50 mmol/L imidazole, pH 7.4) to remove impurities. The target protein was purified by adding 3−5 mL of elution buffer (50 mmol/L Tris, 300 mmol/L NaCl, 10 mmol/L $CaCl_2$, and 150 mmol/L imidazole at pH 7.4) to the column. Protein purity and the level of Bt-HepI expression were confirmed using sodium dodecyl sulfate polyacrylamide gel electrophoresis. SDS-PAGE was used to assess the level of Bt-HepI expression, and the Bradford assay was performed to determine the protein concentration[31].

Site-directed mutagenesis of the Bt-HepI gene was performed *via* PCR using pE-SUMO-Bt-HepI as a template and the Vazyme Quick Change kit. The mutated genes were subjected to DNA sequencing using GeneWise Biotechnology Co., Ltd. (China). The correct mutants were transformed into *E. coli* BL21 (DE3) cells for protein expression. The primer sequences used in site-directed mutagenesis are listed in Table 1.

2.5 Determination of enzyme activity, enzymatic properties, kinetic parameters, and thermostability of HepI

HepI activity was measured at 232 nm[32]. Heparin was used as the substrate in the reaction, which was performed at 30 ℃ for 10 min in a reaction buffer comprised of 25 g/L of heparin, 50 mmol/L CH_3COONa, and 5 mmol/L $Ca(CH_3COO)_2$ at pH 7.4 (pH adjusted to 7.4 using HCl). A ultraviolet (UV) spectrophotometer was used to detect the absorption of heparin at 232 nm. A molar extinction coefficient of 3 800 L/(mol·cm) was used to calculate heparin activity. The amount of enzyme required to catalyze the conversion of 1 μmoL of substrate to product per minute under optimal reaction conditions is designated as 1 international unit (IU).

The optimal pH of the enzyme was measured by determining its activity at pH ranging from 4 to 12 (pH 4−6, citrate buffer; pH 6−8, phosphate buffer; pH 8−12, Tris-HCl). Enzyme activity at the optimum pH was defined as 100%, and the relative enzyme activity of HepI was determined. Enzyme activity was measured at 25, 30, 35, 40, 45, 50, and 55 ℃ to determine the optimum reaction temperature. Enzyme activity at the optimum temperature was defined as 100%, and the relative enzyme activity of HepI was determined.

The kinetic parameters of Bt-HepI (michaelis-menten (K_m), maximum velocity (V_{max}), catalytic constant (k_{cat}), and k_{cat}/K_m) were determined at optimum pH and temperature. The reaction buffer comprised 25 g/L heparin, 50 mmol/L CH_3COONa, and 5 mmol/L $Ca(CH_3COO)_2$ at pH 7.4 (pH adjusted to 7.4 using HCl). The reaction time was 10 min. Eadie-Hofstee plots were used for calculating the K_m and V_{max} values. The half-life ($t_{1/2}$) of purified wild-type and mutant Bt-HepI was determined by incubation at 40 and 50 ℃ for different durations. The enzyme activity before incubation was defined as 100%.

2.6 Preparation and mass spectrometry analysis of LMWH

The protocol for the LMWH preparation using both wild-type and mutant enzymes was performed as follows. In the enzyme digestion process for sample preparation, heparin 50 mg was dissolved in 500 μL of 50 mmol/L Tris-HCl (containing 10 mmol/L $CaCl_2$, pH 7.4) and added to 4 IU of purified HepI in a water bath at 40 ℃ for 12 h. The enzyme was inactivated by boiling in a water bath at 100 ℃ and centrifuging to obtain the supernatant. The supernatant was amended with sodium chloride to a final concentration of 2.5% and, 1.4 times ethanol (*m*/*m*), and left at 4 ℃ for 24 h. After 24 h of centrifugation, the precipitate was dried, and the enzyme digestion product was obtained. Degraded LMWH was analyzed using an oligosaccharide time-of-flight mass spectrometry[33]. A steel target plate was used, the matrix solution contained 2,5-dihydroxy benzoic acid (20 mg/L, 30 ℃ dissolved), and 1 mmol/L NaCl as the matrix additive. The sample was dissolved in 30% acetonitrile (1 mg/mL). The analyzed

Table 1
Oligonucleotide primer pairs used to construct the mutant enzymes.

Sample No.	Amino acid change	Primer sequences[a]
1	Q198R	5′-CTGGATAAG**CGG**GGCAACCCGGTTAAGGACAAGAATG-3′ 5′-CGGGTTGCC**CCG**CTTATCCAGGCGTGCAACTTTCTC-3′
2	K247W	5′-AGCGATCGC**TGG**TGGCTGACCGATAAAGACGACCGTTG-3′ 5′-GGTCAGCCA**CCA**GCGATCGCTGTTGGCTTTGATGTAG-3′
3	H189W	5′-ACGTTGGC**TGG**GAGAAAGTTGCACGCCTGGATAAGC-3′ 5′-CAACTTTCTC**CCA**GCCAACGTTCTTTTTAAAAAAGG-3′
4	D204C	5′-CCGGTTAAG**TGC**AAGAATGGCAAGCCGGTGTATAAAG-3′ 5′-GCCATTCTT**GCA**CTTAACCGGGTTGCCCTGCTTATC-3′
5	K208C	5′-AAGAATGGC**TGC**CCGGTGTATAAAGCAGGCAAGCCG-3′ 5′-ATACACCGG**GCA**GCCATTCTTGTCCTTAACCGGGTTG-3′

Note: [a]Base changes in the relevant triplets are shown in bold.

sample solution contained 1 μL of sample solution and 1 μL of matrix solution and was naturally dried on the sample target.

2.7 Potency testing of enzymatic digestion products

The anti-factor Xa (FXa) and anti-factor IIa (FIIa) activities of LMWH were determined using a protocol from the European Pharmacopoeia[34]. This method determines the ability of the sample to inhibit factors Xa and IIa by comparing the *in vitro* antithrombin activity of the sample with the LMWH standard. The reaction was performed on a microplate reader. The samples were successively mixed with the R1, R2, and R3 (buffers in the kit). The reaction was terminated by adding a citric acid solution; absorbance was measured at 405 nm[35].

2.8 Statistical analysis

Bt-HepI and heparin were molecularly docked using the AutoDock software. PyMOL was used to create all structure maps (hppt://www.pymol.org)[36]. Three parallel runs of the tests were conducted. The results are presented as the mean ± standard deviation. Statistical analyses were performed using *t*-tests.

3. Results

3.1 Workflow for the directed evolution of a HepI

In this study, we adopted 2 strategies to improve the thermal stability of Bt-HepI. The first method involved a virtual mutation of the flexible region in Bt-HepI through MDs to screen for potential mutation sites. In addition, a virtual mutation of disulfide bonds was performed on Bt-HepI to increase the disulfide bond to increase the heat stability. Fig. 1 shows the workflow for the directed evolution of the designed HepI. The workflow progressed from the initial molecular docking of enzyme and substrate to MDs and virtual mutation screening of disulfide bonds to identify key amino acid residues affecting the thermal stability of HepI, to the construction and experimental validation of various mutants. The structural simulation was followed by experimental verification and regression to structural analysis.

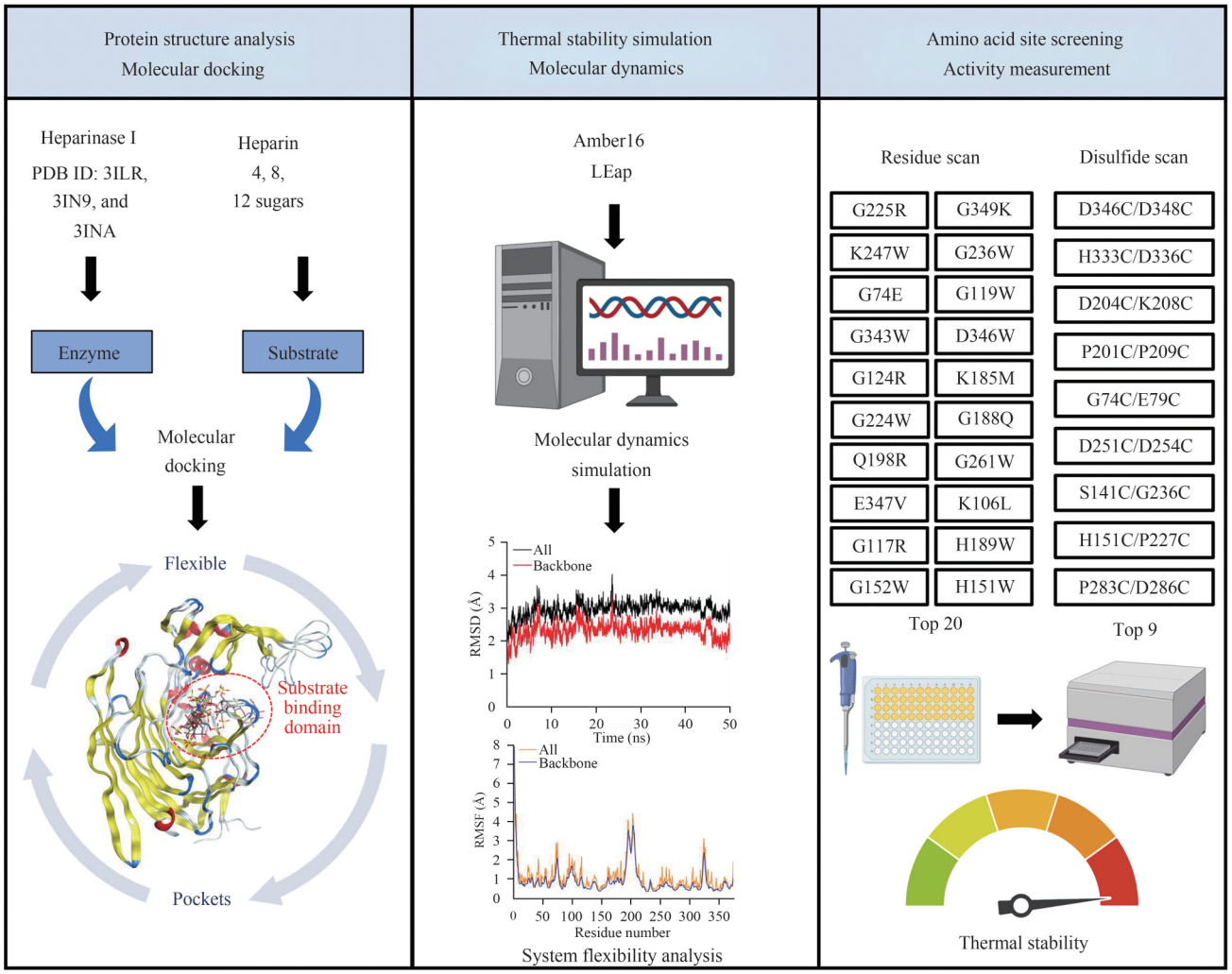

Fig. 1 Crystal structure of the existing HepI was overlaid while molecularly docking it to the heparin to determine the substrate binding pocket (active center region) of the enzyme. MDs of HepI were performed using Amber16 to identify amino acid residues associated with thermal stability. Virtual mutation screening of HepI using the Residue and Disulfide modules of Amber16 identidied mutations in key amino acid residues for functional validation *via* high temperature thermal stability experiments.

3.2 Rational design strategy for enhanced thermal stability

To obtain highly active and thermally stable Bt-HepI, MD flexibility disulfide bonding analyses were performed. The selected flexible areas include positions 70−80, 180−225, and 320−330 (Fig. 2A). As amino acids 70−80 were very close to the catalytic center, the flexible region containing amino acids 70−80 was deemed unsuitable for the mutation to avoid any effects on the enzyme activity. The flexible areas of residues 180−225 and 320−330 were considered the best residues for the mutation (Fig. 2B). The top 20 structural positions of the screened flexible mutant amino acid sites and mutation energy are shown in Figs. 2C-D. A simulated screening of the disulfide bonds was performed to avoid the active site of the enzyme. The structural position of the disulfide bond mutation site top 9 is shown in Fig. S1. After further analysis and excluding of the active center, only 4 disulfide bond mutation sites remained (P283C/D286C, S141C/G236C, P201C/P209C, and D204C/D208C), as shown in Fig. 3.

3.3 Analysis of relative enzyme activity, expression of mutants, and sequence analyse

Enzyme activity was measured for the 20 single-point mutants and four disulfide bond mutants screened. The mutants H189W, Q198R, K247W, and D204C/K208C did not show a significant decrease in enzyme activity compared with that seen with the wild type (Figs. 4A-B). H189W, Q198R, and D204C/K208C showed higher enzyme activity than the wild-type, and mutant K247W showed lower activity than the wild-type. Therefore, we subsequently selected the, H189W, Q198R and D204C/K208C mutation sites, for combinatorial mutagenesis (H189W/Q198R, H189W/D204C/K208C, Q198R/D204C/K208C and H189WQ198R/D204C/K208C) to obtain highly active and thermally stable HepI. Eight mutants of Bt-HepI expressed soluble enzymes (Fig. 4C). The activities of these enzymes were determined, as shown in Fig. 4D. Compared with the wild-type, the enzyme activity of 7 mutants remained unchanged or was significantly increased. Bt-HepI^{K247W} was an exception and exhibited, decreased activity. The sequences of the Bt-HepI and polysaccharide lyase family 13 enzymes were compared and analyzed, and 5 beneficial mutation sites were also determined. The 5 sites that were experimentally mutated are marked by the 5-pointed stars (Fig. S2). Except for amino acid residue 208, other residues were highly conserved among all investigated enzymes. The total yield, total enzyme activity, and specific enzyme activity of wild-type and mutant Bt-HepI enzymes were determined (30 °C , reaction buffer comprised of 25 g/L of heparin, 50 mmol/L CH_3COONa, and 5 mmol/L $Ca(CH_3COO)_2$ at pH 7.4). The expression levels of all the mutants remained consistent compared with that seen with the wild type and did not differ significantly. However, mutants D204C/K208C and D204C/K208C/H189W/

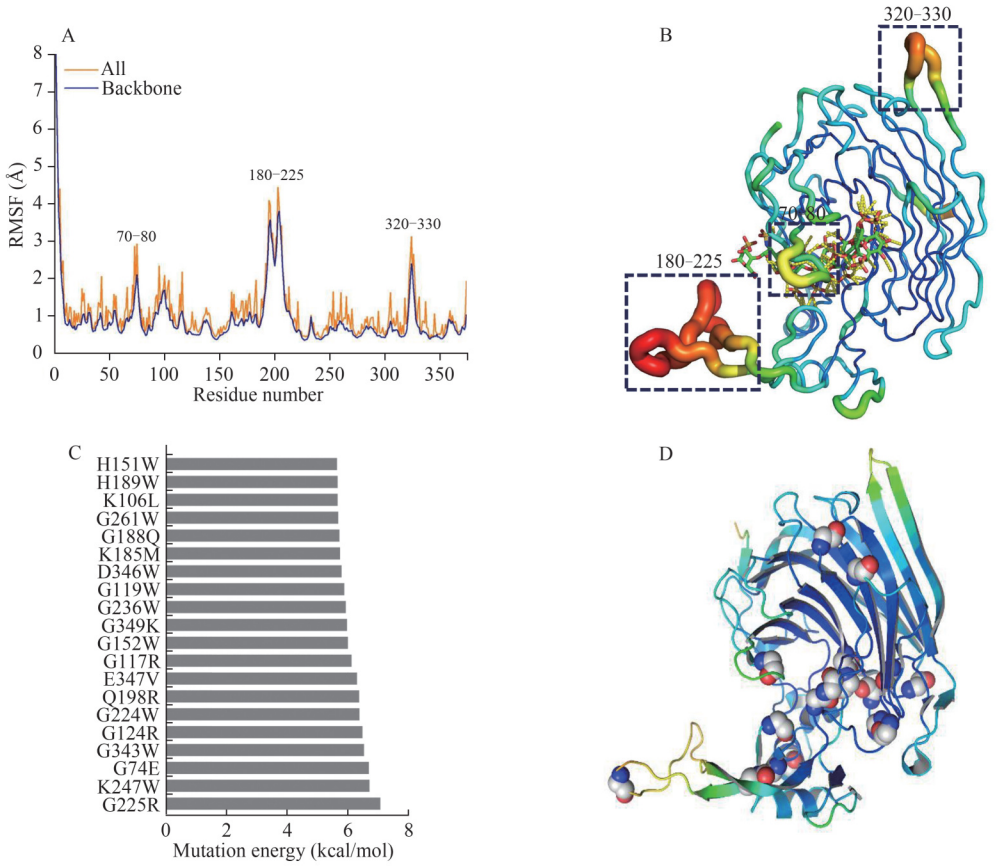

Fig. 2 Molecular dynamics simulation and virtual mutation screening of HepI. (A) RMSF calculations using Amber16 were used to determine the flexibility of the protein regions by comparing the framework conformation with the average conformation and the RMSD size of each amino acid. The 3 regions with better flexibility were residues 70−80, 180−225 and 320−330. (B) Spatial display of flexible regions. The redder and thicker the line, the greater flexibility of the area. The more flexible areas are the 3 dashed. (C) Mutation energy analysis of the top 20 loci of single point virtual mutations. (D) The top 20 structural positions of flexible mutant amino acid sites were screened. Amino acid residues are indicated using globular structures.

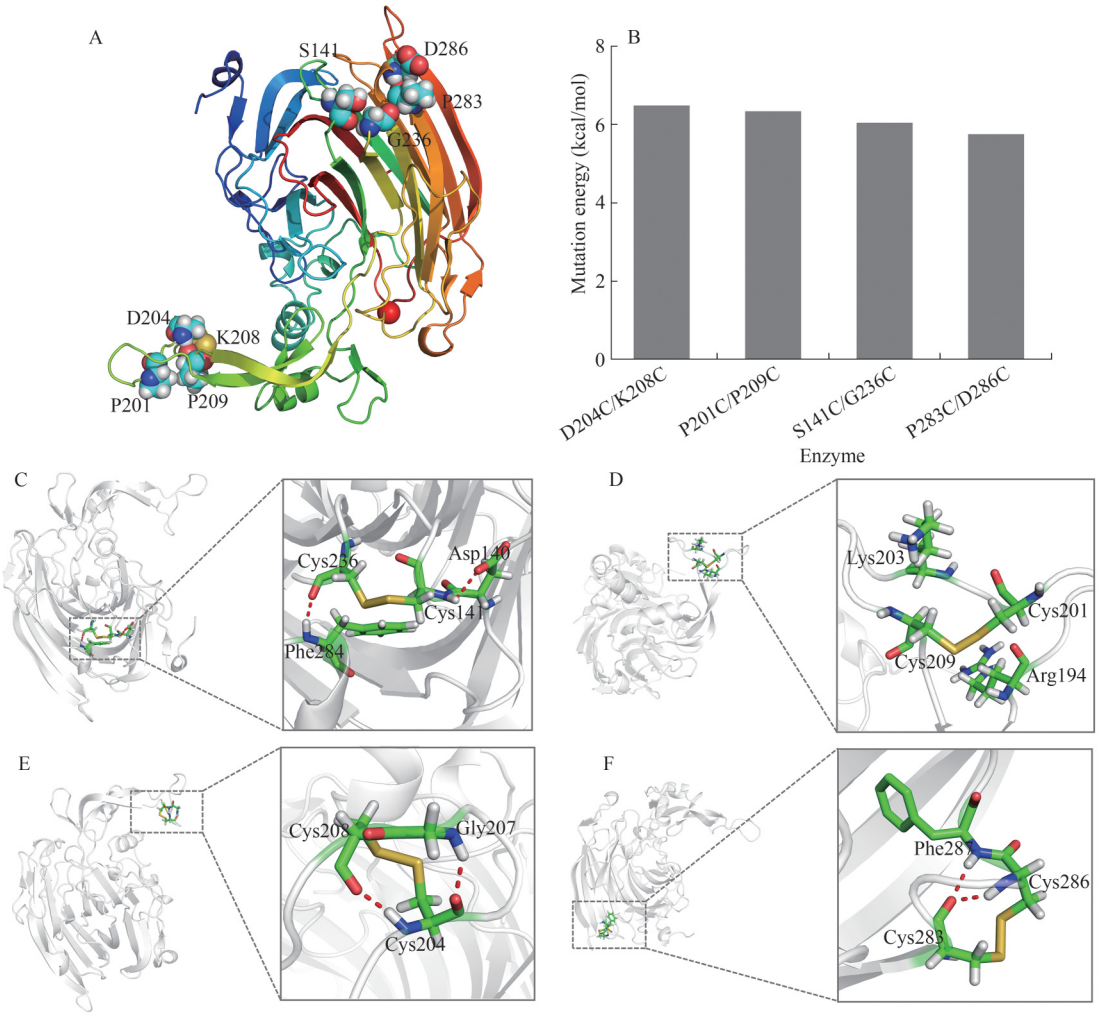

Fig. 3 Schematic structure of the four disulfide bond mutation sites outside the active center of HepI. (A) Fours pairs of structural positions of disulfide-bonded mutant amino acid sites were screened, amino acid residues are indicated using globular structures. (B) Mutation energy analysis of the top 20 loci of single point virtual mutations. (C-F) Disulfide bond between the amino acid residues at positions (C) 236 and 141, (D) 201 and 209, (F) 204 and 208, 283 and 286.

Q198R had significantly higher specific enzyme activities than the wild type (Table 2). This occurs probably because the wild-type enzyme loses more of its catalytic activity at the assay temperature conditions.

3.4 Analysis of Bt-HepI mutants for enzymatic properties, thermal stability, and enzyme kinetics

We determined the optimal reaction temperature and pH for each mutant by comparing relative activities at various temperatures and pH levels (Fig. S3). The optimum reaction pH for Bt-HepI^{WT}, Bt-HepI^{K247W}, Bt-HepI$^{D204C/K208C}$, and BtHepI$^{D204C/K208C/H189W}$ was the same (pH 8). When His was mutated to Trp, increasing acidity, the optimal pH of Bt-HepI^{H189W} changed from pH 8 to pH 7. As Arg is a basic amino acid, when Q198 was mutated to R198, the optimal pH of the mutants (Bt-HepI^{Q198R}, Bt-HepI$^{H189W/Q198R}$, Bt-HepI$^{D204C/K208C/Q198R}$, Bt-HepI$^{D204C/K208C/H189W/Q198R}$) changed from pH 8 to pH 9. The optimum reaction temperature of Bt-HepI^{WT}, Bt-HepI$^{D204C/K208C}$, and Bt-HepI^{K247W} were 40 °C, whereas the optimal reaction temperature for the remaining mutants is 40−45 °C. Overall, mutations in amino acid residues altered the flexibility of the enzyme and increased its rigidity, leading to a higher optimal reaction temperature.

To confirm the thermostability of the mutants, their half-life at 40 and 50 °C were measured. The optimal temperature for Bt-HepI was 40 °C. Thus, 50 °C was a relatively high temperature for Bt-HepI. Bt-HepI^{WT} lost half its enzymatic activity at 50 °C in a short time. The half-life of each mutant was significantly higher than that of Bt-HepI^{WT}, indicating that these mutations improved the thermal stability of Bt-HepI (Figs. 5A-B). Compared with the wild-type enzyme, the half-life of 8 Bt-HepI mutants (Bt-HepI^{Q198R}, Bt-HepI^{K247W}, Bt-HepI^{H189W}, Bt-HepI$^{D204C/K208C}$, Bt-HepI$^{H189W/Q198R}$, Bt-HepI$^{D204C/K208C/H189W}$, Bt-HepI$^{D204C/K208C/Q198R}$, and Bt-HepI$^{D204C/K208C/K208C/H189W/Q198R}$) increased by 30.55%, 14.63%, 31.39%, 51.61%, 56.61%, 74.07%, 80.77%, and 104.35% at 40 °C and, 61.03%, 30.82%, 72.21%, 101.32%, 103.32%, 113.75%, 122.81%, and 143.5% at 50 °C, respectively.

We attempted to identify mutations that would improve the thermal stability of Bt-HepI by using mutation sites that were not in the active region of the enzyme. The enzyme kinetic constant and half-life of each mutant were determined to identify the best mutant (Table 3). The catalytic constant of Bt-HepI^{K247W} was 17.9% higher than that of the wild-type, and the K_m values of the other mutants were lower, indicating the enhanced binding ability of the mutants to

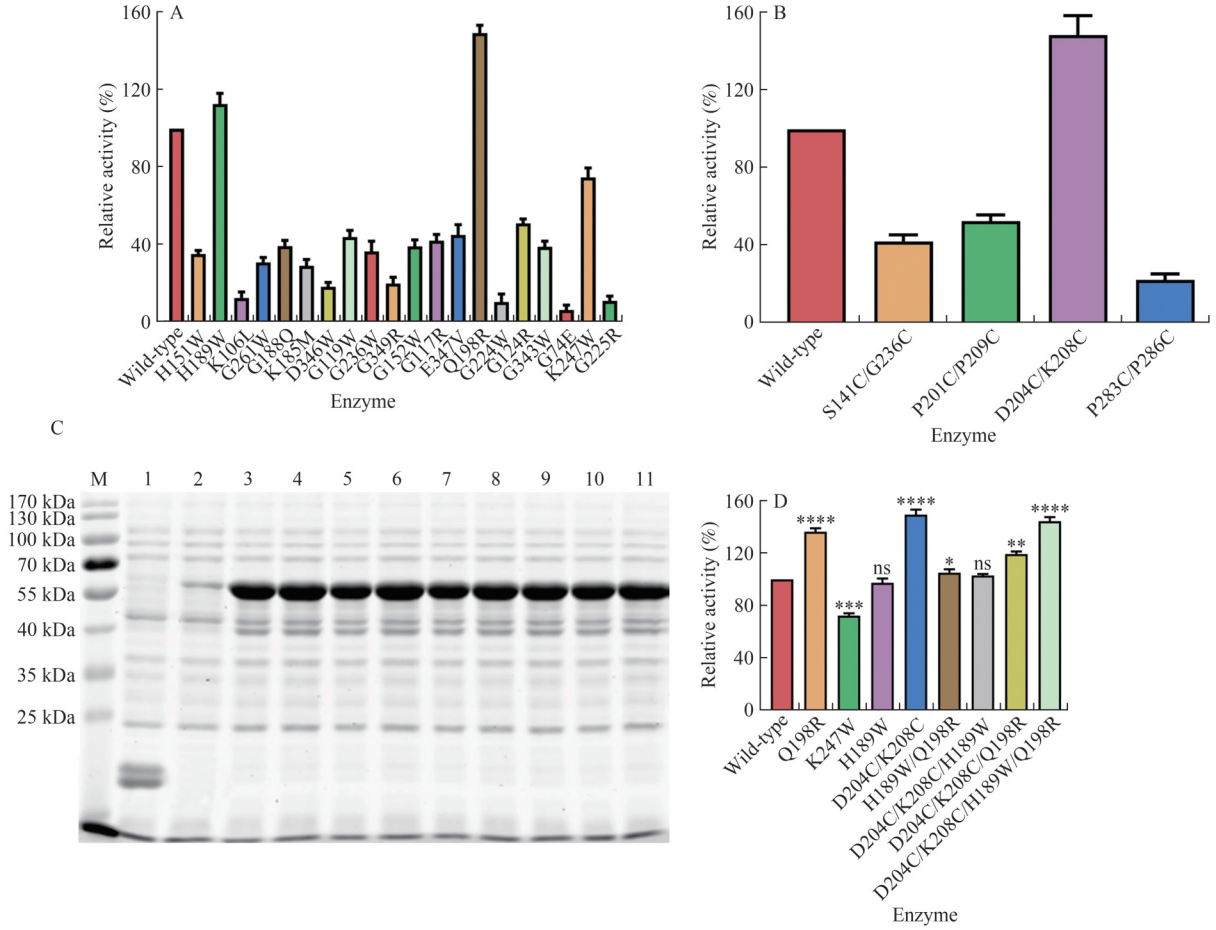

Fig. 4 Comparison of mutation energy and enzyme activity of mutants. Expression of wild-type and mutant proteins was analyzed using 12% SDS-PAGE gels stained with Kaomas Brilliant Blue R-250. (A-B) Comparison of the activity of single point mutations (top 20) and disulfide bond mutations. The enzyme activity of the wild-type enzyme was considered 100%. Mutants H189W, Q198R and D204C/K208C had higher activity than the wild type, and K247 had slightly lower activity than the wild type. (C) Lane M: protein marker; Lanes 1 and 2: recombinant strains with empty plasmid and wild-type enzyme without induction, respectively. Lanes 3-11: wild-type Bt-HepI and Q198R, K247W, H189W, D204C/K208C, H189W/Q198R, D204C/K208C/H189W, D204C/K208C/Q198R, and D204C/K208C/H189W/Q198R Bt-HepI mutants produced by inducing recombinant bacteria. The Bt-HepI protein band was approximately 55 kDa. Sample volume of 25 μL/well. (D) Relative enzyme activity analysis of the mutants. The enzyme activity of the wild-type enzyme was considered 100%. All experiments comprised 3 parallel groups for SD analysis. ns, $P > 0.05$; *$P < 0.05$; **$P < 0.01$; ***$P < 0.001$; ****$P < 0.000\ 1$.

Table 2
Enzyme activity and yield of wild type Bt-HepI and mutants.

Enzyme	TP (mg/mL)	TEA (IU/mL)	SA (IU/mg)
Wild-type	0.31 ± 0.02	62.0 ± 1.4	200.0 ± 8.3
Q198R	0.41 ± 0.04	85.0 ± 2.7	206.0 ± 10.2
K247W	0.29 ± 0.01	45.0 ± 1.9	157.0 ± 5.6
H189W	0.32 ± 0.03	61.0 ± 3.2	190.0 ± 6.3
D204C/K208C	0.42 ± 0.06	93.0 ± 3.9	222.0 ± 7.5*
H189W/Q198R	0.33 ± 0.07	66.0 ± 2.7	198.0 ± 5.7
D204C/K208C/H189W	0.30 ± 0.02	64.0 ± 1.3	212.0 ± 6.3
D204C/K208C/Q198R	0.36 ± 0.05	75.0 ± 2.0	209.0 ± 5.4
D204C/K208C/H189W/Q198R	0.39 ± 0.04	90.0 ± 3.1	230.0 ± 4.9**

Note: TP, total protein; TEA, total enzyme activity; SA, specific activity. Significant differences are compared with wild-type, *$P < 0.05$, **$P < 0.01$.

the substrate, except for Bt-HepI^{K247W}. In addition, the k_{cat} of all Bt-HepI mutants, except Bt-HepI^{K247W}, was significantly higher than that of Bt-HepI^{WT}. The Bt-HepI mutants were similar to Bt-HepI^{WT} for all evaluated parameters. Therefore, the mutants improved the thermal stability of the enzyme and increased its catalytic efficiency.

3.5 Structural analysis of mutants

To investigate the effects of amino acid mutations on thermal stability, spatial three-dimensional structures of Bt-HepI^{Q198R}, Bt-HepI^{K247W}, Bt-HepI^{H189W}, and Bt-HepI$^{D204C/K208C}$ were systematically analyzed. Fig. 5C shows the structural analysis results for Bt-HepI^{Q198R}. When Q198 was mutated to R198, the side-chain aromatic nucleus extended away from the protein. By creating cation-stacking contacts with the protonated amino ion of the nearby K197, this stretched aromatic nucleus exhibited a conjugated effect that further stabilized this flexible area and increased the heat stability of the mutant. Structural analysis of Bt-HepI^{K247W}, in which K247 was mutated to W247, revealed a conjugated effect *via* the formation of π-π stacking interactions, which improved the thermal stability of this mutant. Spatially, W247 and Y273 were aligned, exerting a conjugated effect *via* π-π stacking interactions because of, the aromatic nuclei in both molecules. In the spatial structure analysis of Bt-HepI^{H189W} with H189 mutated to W189, a side-chain aromatic nucleus appeared above K184, which had a conjugation effect by forming cation-π stacking interactions between the protonated amino ions of K184. The

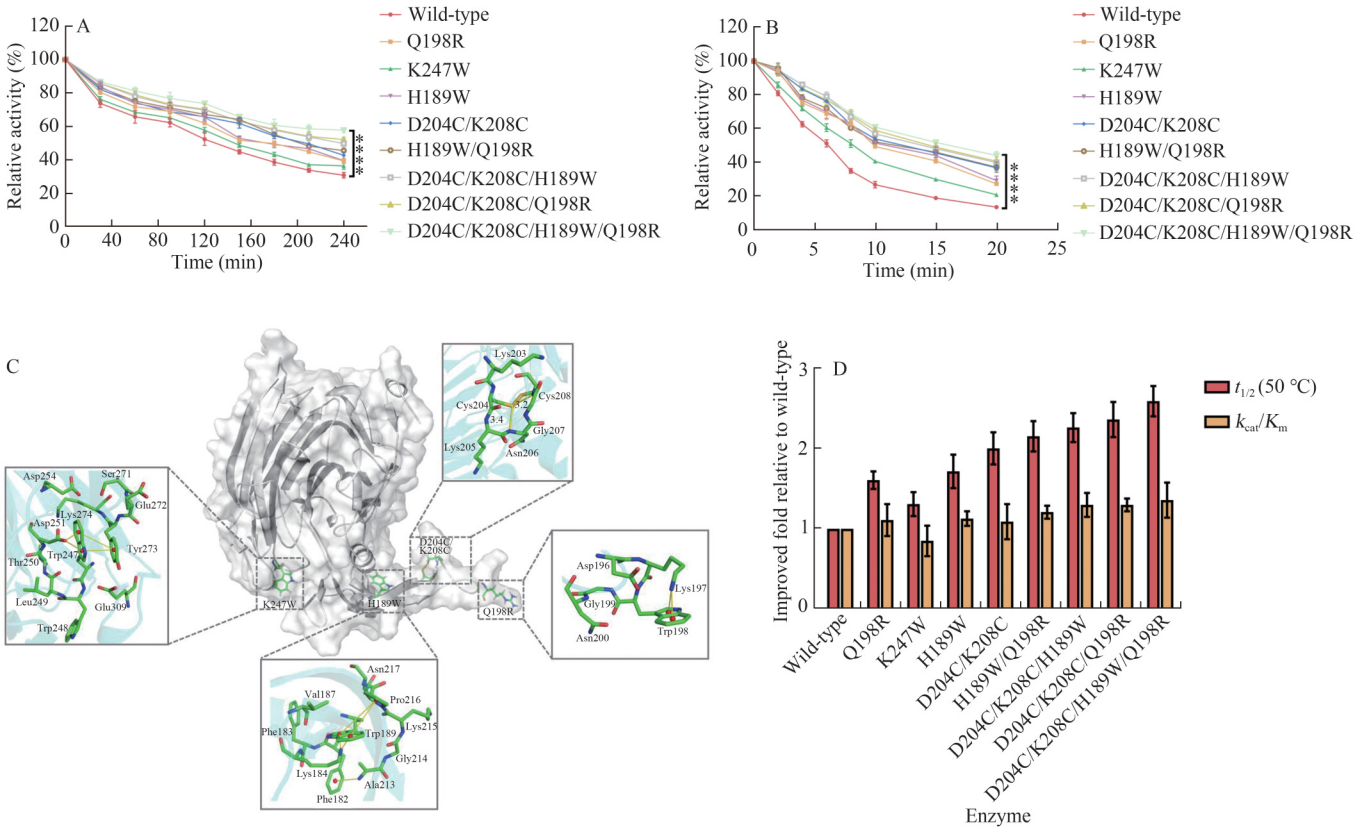

Fig. 5 Structure of Bt-HepI wild-type and mutant enzymes, and catalytic efficiency and half-life analysis. Temperatures of (A) 40 °C and (B) 50 °C were used. The initial enzyme activity of different Bt-HepI mutants was set to 100%, and the enzyme activity at different treatment times was compared to obtain the remaining activity. The thermal stability of the best mutant (D204C/K208C/H189W/Q198R) was significantly higher than that of the wild type. The half-life at 40 and 50 °C were 2.04 and 2.44 times higher than those of the wild type, respectively. Three independent experiments were performed in parallel for each data set. Statistical analyses and graphing were performed. (C) In the H189W mutant, when H189 mutated to W189, a side-chain aromatic nucleus presented above K184, producing a conjugated effect by forming cation-π stacking interactions between the protonated amino ions of K184. In the Q198R mutant, when Q198 mutated to R198, a side chain aromatic nucleus extended away from the protein, with a conjugated effect because of the induction of a cation-π stacking interaction with the protonated amino ion of the adjacent K197. In the K247W mutant, when K247 mutated to W247, a conjugated effect occurred because of the induction of a π-π stacking interaction, which improved the thermal stability of this mutant. K247W and Y273 correspond spatially, thereby having a conjugated effect by forming π-π stacking interactions as they both have aromatic nuclei. In the D204C/K208C mutant, the mutant forms a disulfide bond at positions 204 and 208. Residues C204 and C208 form a disulfide bond and, hydrogen bonds with D206 and G207. The co-action of the disulfide and hydrogen bonds makes this flexible region more stable in the D204C/K208C mutant. (D) Fold increase in catalytic efficiency and 50 °C half-life of the mutant compared with that of wild-type.

Table 3
Kinetic parameters and stability properties of wild type Bt-HepI and mutants.

Enzyme	K_m (mmol/L)	V_{max} (mmol/(L·min))	k_{cat} (s^{-1})	k_{cat}/K_m (L/(mmol·s))	$t_{1/2}$ (40 °C) (min)	$t_{1/2}$ (50 °C) (min)
Wild-type	0.16 ± 0.02	0.20 ± 0.04	78.0 ± 4.9	486 ± 16	147.0 ± 1.2	6.6 ± 0.3
Q198R	0.16 ± 0.03	0.21 ± 0.05	83.0 ± 6.3	520 ± 18	193.0 ± 1.3	10.7 ± 0.5
K247W	0.19 ± 0.04	0.19 ± 0.06	78.0 ± 5.1	409 ± 23	169.0 ± 1.0	8.7 ± 0.2
H189W	0.16 ± 0.01	0.22 ± 0.03	87.0 ± 4.6	543 ± 18	194.0 ± 1.3	11.4 ± 0.7
D204C/K208C	0.16 ± 0.02	0.23 ± 0.02	82.0 ± 6.7	511 ± 24	224.0 ± 2.3	13.3 ± 0.4
H189W/Q198R	0.15 ± 0.03	0.21 ± 0.04	88.0 ± 7.1	589 ± 28	231.0 ± 1.6	13.5 ± 0.4
D204C/K208C/H189W	0.15 ± 0.01	0.24 ± 0.03	92.0 ± 5.3	612 ± 31	257.0 ± 1.7	14.2 ± 0.7
D204C/K208C/Q198R	0.15 ± 0.02	0.24 ± 0.04	93.0 ± 6.3	618 ± 29	267.0 ± 1.8	14.8 ± 0.6
D204C/K208C/H189W/Q198R	0.14 ± 0.02	0.25 ± 0.03	93.0 ± 4.7	667 ± 28	301.0 ± 1.5	16.1 ± 0.5

Bt-HepI^{H189W} improved the thermal stability of the enzyme for the same reason as the Bt-HepI^{Q198R}. Structural analysis showed that in Bt-HepI$^{D204C/K208C}$, disulfide bonds formed at positions 204 and 208, which markedly affected the thermal stability of this mutant. Residues C204 and C208 formed disulfide and hydrogen bonds with D206 and G207. The co-action of disulfide and hydrogen bonds led to a more stable and flexible region in Bt-HepI$^{D204C/K208C}$. Based on these results, the combined mutation had a more pronounced effect than a single point mutation. The catalytic efficiency of all mutants remained the same or was increased compared with that of the wild-type enzyme

(Fig. 5D). However, the half-life of the mutants at 50 ℃ were significantly higher. The most significant improvement in thermal stability was observed for Bt-HepI$^{D204C/K208C/H189W/Q198R}$.

3.6 Mass spectrometry and activity determination of LMWH

To study the degradation of heparin by the mutated enzyme, we performed mass-spectrometry and activity measurements of the degradation products. A previous study demonstrated that Bt-HepI degrades heparin in LMWH[37]. We measured the mass spectra of the enzymatic hydrolysates at 40 ℃ for wild-type and mutants (Table 4). For specific original Mass spectrometry raw data, see Supplementary Material Fig. S4. Compared with the LMWH standards, the average molecular weight of the enzymatic digestion products of the wild-type and mutant H189W was higher than that required by the standard; however, the remaining were consistent with the standard (4 000−5 500 Da). The anti-FXa and anti-FIIa activities of the enzymatic digests determined using the chromogenic substrate method are shown in Table 4. The anti-FXa and anti-FIIa activities of the wild-type were lower than the pharmacopoeial standard requirements of 1.5−2.5 compared with that of LMWH, whereas the rest of the mutants met the requirements[38].

4. Discussion

Many heparinases have been isolated from the gut microbiota, and the heparin-degrading bacterium HJ-15 was isolated from human feces[39]. The highly active HepI of *B. cellulosilyticus* has been cloned and expressed[17]. However, studies to improve the thermal stability of HepI based on its crystal structure have not been reported. Rational protein engineering has proven to be the most versatile and comprehensive strategy for engineering industrial biocatalysts. Therefore, the crystal structure of HepI must be thoroughly explored to improve its thermal stability and to modify the regions of the enzyme that exhibit poor stability. When designing heat-resistant proteins, the flexible instability regions of the proteins must be identified. Once weak spots are identified, further thermostability can be achieved by optimizing the weak spot regions[40]. However, the relationship between flexibility, stability, and mobility is complex. Many proteins in the folded state must be flexible to perform their functions, such as binding ligands, regulating enzyme activity, and interacting with macromolecules[41]. A study of polyethylene terephthalate (PET)-degrading enzymes identified the final IsPETase$^{S121E/D186H/R280A}$ variant by virtual mutation screening of the enzyme molecule with good thermal stability[42]. A recent study described the addition of a pair of disulfide bonds (N233C/S282C) to the DuraPET enzyme to improve thermal stability[43]. This study was based on a virtual mutation screen of Amber16 for heat stability mutation site selection. We determined the flexible amino acid residues and disulfide bond formation sites of Bt-HepI using computer simulation calculations. *D*-stability was calculated by virtually screening the mutations (Figs. 2C and 3B). Compared to the thermal stability of the Bt-HepI^{WT}, that of the Bt-HepI$^{D204C/K208C/H189W/Q198R}$ was significantly improved (Table 3). We partitioned the flexible region of HepI in the simulation calculation by excluding amino acids at positions 70−80 of the flexible region in the active region. Amino acid mutations in this region may affect binding between the substrate and enzyme molecules, thereby affecting enzyme activity (Fig. 2B). Mutations in flexible amino acids on the surface of the enzyme molecule may also alter enzyme activity and solubility. Therefore, specific Bt-HepI mutants were recombinantly expressed, and their total enzyme activity, specific enzyme activity, and yield were determined (Table 2). The catalytic constant of only Bt-HepI^{K247W} was higher than that of Bt-HepI^{WT}; the K_m values of the other mutants were lower than those of Bt-HepI^{WT}, and the k_{cat} values increased compared with those of Bt-HepI^{WT}. These results indicate that the mutants had better thermal stability and activity than Bt-HepI.

Early research evaluated, the optimal temperature and pH values for extracting HepI from *Flavobacterium heparinase*. The optimal temperature and pH values of the wild-type and mutant Bt-HepI enzymes were consistent with previous findings[35]. Many studies have been conducted on the expression of fusion proteins and modifications of HepI; however, no significant changes were observed in the optimal temperature or pH[37,44-45]. In this study, mutations involved amino acid residues associated with enzyme thermal stability; the optimum pH and temperature of the mutants varied. A carboxyl group was added to Bt-HepI^{K247W} when it mutated from K247 to W247, causing bias toward an acidic environment, and the optimum pH changed from pH 8 to pH 7. As Arg is a basic amino acid and tends to be stable in alkaline environments, the optimal reaction pH of Bt-HepI^{Q198R}, Bt-HepI$^{H189W/Q198R}$, Bt-HepI$^{D204C/K208C/Q198R}$, and Bt-HepI$^{D204C/K208C/H189W/Q198R}$ changed from pH 8 to pH 9. The optimum pH of Bt-HepI^{H189W}, Bt-HepI$^{D204C/K208C}$, and Bt-HepI$^{D204C/K208C/H189W}$ did not differ from those of Bt-HepI^{WT}. We assessed the structure of Bt-HepI to improve the thermal stability of the enzyme molecules. Compared with the optimum reaction temperature of Bt-HepI^{WT}, those of

Table 4
Determination of anticoagulant activity and molecular weight of enzymatic digestion products at 40 ℃.

Sample	Anti-FXa (IU/mg)	Anti-FIIa (IU/mg)	Anti-FXa/Anti-FIIa	Relative molecular mass
LMWH	122.0 ± 3.5	48.0 ± 5.0	2.5 ± 0.2	4 428.87
Wild-type	87.0 ± 7.8	85.0 ± 3.6	1.0 ± 0.1	8 168.03
Q198R	118.0 ± 7.0	56.0 ± 4.0	2.1 ± 0.1	4 589.78
K247W	115.0 ± 5.7	57.0 ± 5.0	2.0 ± 0.1	4 811.84
H189W	117.0 ± 4.7	55.0 ± 3.9	2.1 ± 0.2	4 723.49
D204C/K208C	120.0 ± 3.7	53.0 ± 4.9	2.3 ± 0.2	4 856.97
H189W/Q198R	116.0 ± 5.3	55.0 ± 5.3	2.1 ± 0.2	4 679.41
D204C/K208C/H189W	120.0 ± 3.0	54.0 ± 2.2	2.2 ± 0.2	4 589.78
D204C/K208C/Q198R	121.0 ± 3.5	55.0 ± 2.9	2.2 ± 0.1	4 592.97
D204C/K208C/H189W/Q198R	120.0 ± 4.5	54.0 ± 3.0	2.2 ± 0.1	4 503.95

Note: Samples were enzymatic digestion products.

Bt-HepI^{Q198R}, Bt-HepI^{H189W}, Bt-HepI$^{H189W/Q198R}$, Bt-HepI$^{D204C/K208C/H189W}$, Bt-HepI$^{D204C/K208C/Q198R}$, and Bt-HepI$^{D204C/K208C/H189W/Q198R}$ changed from 40 to 45 ℃. This increase occurred because of a change in the flexibility of the mutant proteins, leading to a more stable structure, which ultimately affected the reaction temperature. In a study for the thermal stability of MBP-HepI, C297 was replaced by S297, and the total enzyme activity increased by 30.6%[19]. Currently, only the structure of HepI, which includes the enzyme active domain and region where Ca^{2+} binds to *Bacteroides*, has been investigated[18]. The thermal stability of HepI remains to be analyzed. Based on the structure of the enzyme molecule, the unstable region of HepI was identified through computer simulation. According to virtual mutation screening and active site analysis, the best mutation was rationally designed, and Bt-HepI mutants with high stability were produced. Based on protein structure, the mutant was also analyzed to improve the thermal stability of the enzyme.

Here, we investigated the structure of Bt-HepI to determine the reasons for the increased thermal stability of the mutant. π-Stacking is widely observed in biological macromolecular systems and often plays a key role in maintaining specific protein structures and recognizing protein-ligand interactions[46-47]. The main forms of π-π stacking include π-π, cation-π, anion-π, halogen bond-π and CH-π stacking. Three mutants, Bt-HepI^{Q198R}, Bt-HepI^{K247W}, and Bt-HepI^{H189W}, formed cation-π and π-π stacking interactions in their local regions, which markedly increased the protein stability (Fig. 5C). Disulfide bonds force close positioning of the amino acid residues of the same peptide chain. Thus, the peptide chains fold rapidly and form a stable spatial topology. Further, hydrophobic amino acid residues surround the disulfide bonds, which can form a local hydrophobic center region to prevent water molecules from entering the peptide and disrupting the hydrogen bonds. Therefore, disulfide bonds are conducive to the formation of stable, high-level structural regions and play key roles in protein folding and stability[48-49]. Through virtual screening of disulfide bonds, we found that Bt-HepI$^{D204C/K208C}$ exhibited high activity and stability. Eventually, we obtained the combinatorial mutant Bt-HepI$^{D204C/K208C/H189W/Q198R}$, whose half-life increased 2.44-fold at 50 ℃ compared with that of the wild-type. The mutant displayed increased activity in experiments. The average molecular weight of the enzymatic digestion products of mutant Bt-HepI$^{D204C/K208C/H189W/Q198R}$ at 40 ℃ was 1.8-fold lower than that of the wild type (Table 4). The main points of the LMWH criteria were met. The success of, our rational protein engineering will contribute to the improvement of HepI stability in the preparation of LMWH from heparin.

5. Conclusion

We developed a Bt-HepI mutant with high thermal stability and high heparin degradation activity using a rational protein engineering strategy. Bt-HepI$^{D204C/K208C/H189W/Q198R}$ showed substantially higher thermal stability and subsequently higher heparin degradation activity than Bt-HepI^{WT}. Compared with that of Bt-HepI^{WT}, the half-life of Bt-HepI$^{D204C/K208C/H189W/Q198R}$ was increased by 2.04- and 2.44-fold at 40 and 50 ℃, respectively. In addition, the k_{cat}/K_m value was 1.3-fold higher for Bt-HepI$^{D204C/K208C/H189W/Q198R}$ than for Bt-HepI^{WT}. The average molecular weight of the prepared LMWH was 1.8 times lower than that of the wild-type, which complies with international pharmacopoeia standards. The low thermal stability of Bt-HepI limits its application for heparin degradation. Thus, our results may contribute to the industrial production of LMWH using HepI. Moreover, information on protein structure can be effectively utilized in rational protein engineering to enhance the thermal stability of a target protein, showing potential for further applications.

Conflict of interest

The authors declare no conflict of interest

Acknowledgements

This work was supported by the Natural Science Foundation of Jiangsu Province (BE2021623, BK20220155); National Natural Science Foundation of China (32001665, U1903205, 32021005); the National Key Research and Development Program of China (2017YF0400303); the Key Scientific and Technological Research Projects in the Key Areas of the Xinjiang Production and Construction Corps (2018AB010); the Key Research and Development 303 Program of Ningxia Province (2020BFG02012); Natural Science Foundation of Jiangsu Province (BE2021623) and Collaborative Innovation Center of Food Safety and Quality Control in Jiangsu Province.

Appendix A. Supplementary data

Supplementary data associated with this article can be found, in the online version, at https://doi.org/10.26599/FSHW.2024.9250134.

References

[1] D.L. Rabenstein, Heparin and heparan sulfate: structure and function, Nat. Prod. Rep. 19 (2002) 312-331. https://doi.org/10.1039/b100916h.

[2] P.S. Damus, M. Hicks, R.D. Rosenberg, Anticoagulant action of heparin, Nature 246 (1973) 355-357. https://doi.org/10.1038/246355a0.

[3] R.D. Rosenberg, L. Lam, Correlation between structure and function of heparin, Proc. Natl. Acad. Sci. U. S. A. 76 (1979) 1218-1222. https://doi.org/10.1073/pnas.76.3.1218.

[4] R. Lever, C.P. Page, Novel drug development opportunities for heparin, Nat. Rev. Drug Discov. 1 (2002) 140-148. https://doi.org/10.1038/nrd724.

[5] G. Torri, A. Naggi, Heparin centenary-an ever-young life-saving drug, Int. J. Cardiol. 212(Suppl 1) (2016) S1-4. https://doi. org/10.1016/S0167-5273(16)12001-7.

[6] Z. Witczak, K. Nieforth, Carbohydrates in drug design, Eur. J. Med. Chem. (1997) 842. https://doi.org/10.1016/S0223-5234(97)82768-7.

[7] H.B. Nader, C.C. Lopes, H.A.O. Rocha, et al., Heparins and heparinoids: occurrence, structure and mechanism of antithrombotic and hemorrhagic activities, Curr. Pharm. Des. 10 (2004) 951-966. https://doi.org/10.2174/1381612043452758.

[8] L. Wang, J.R. Brown, A. Varki, et al., Heparin's anti-inflammatory effects require glucosamine 6-*O*-sulfation and are mediated by blockade of L- and P-selectins, J. Clin. Invest. 110 (2002) 127-136. https://doi.org/10.1172/JCI14996.

[9] C. Zhang, L. Yu, Q. Zhai, et al., *In vitro* fermentation of heparin by the human gut microbiota: changes in the microbiota community and metabolic functions, Food Chem. 406 (2023) 135010. https://doi.org/10.1016/j.foodchem.2022.135010.

[10] H.B. Nader, J.M. Walenga, S.D. Berkowitz, et al., Preclinical differentiation of low molecular weight heparins, Semin. Thromb. Hemost. 25(Suppl 3) (1999) 63-72.

[11] J. Fareed, Q. Ma, M. Florian, et al., Differentiation of low-molecular-weight heparins: impact on the future of the management of thrombosis, Semin. Thromb. Hemost. 30(Suppl 1) (2004) 89-104. https://doi.org/10.1055/s-2004-823007.

[12] D.L. Lohse, R.J. Linhardt, Purification and characterization of heparin

lyases from *Flavobacterium heparinum*, J. Biol. Chem. 267 (1992) 24347-24355.

[13] A. Cartmell, E.C. Lowe, A. Baslé, et al., How members of the human gut microbiota overcome the sulfation problem posed by glycosaminoglycans, Proc. Natl. Acad. Sci. U. S. A. 114 (2017) 7037-7042. https://doi.org/10.1073/pnas.1704367114.

[14] K. Kawai, R. Kamochi, S. Oiki, et al., Probiotics in human gut microbiota can degrade host glycosaminoglycans, Sci. Rep. 8 (2018) 10674. https://doi.org/10.1038/s41598-018-28886-w.

[15] D. Ndeh, A. Baslé, H. Strahl, et al., Metabolism of multiple glycosaminoglycans by *Bacteroides thetaiotaomicron* is orchestrated by a versatile core genetic locus, Nat. Commun. 11 (2020) 646. https://doi.org/10.1038/s41467-020-14509-4.

[16] C.Y. Liu, W.B. Su, L.B. Guo, et al., Cloning, expression, and characterization of a novel heparinase I from *Bacteroides eggerthii*, Prep. Biochem. Biotechnol. 50 (2020) 477-485. https://doi.org/10.1080/10826068.2019.1709977.

[17] L.W. Gao, H.T. Zhu, C.Y. Liu, et al., A highly active heparinase I from *Bacteroides cellulosilyticus*: cloning, high level expression, and molecular characterization, PLoS One 15 (2020) e0240920. https://doi.org/10.1371/journal.pone.0240920.

[18] Y.H. Han, M.L. Garron, H.Y. Kim, et al., Structural snapshots of heparin depolymerization by heparin lyase I, J. Biol. Chem. 284 (2009) 34019-34027. https://doi.org/10.1074/jbc.M109.025338.

[19] S. Chen, F. Ye, Y. Chen, et al., Biochemical analysis and kinetic modeling of the thermal inactivation of MBP-fused heparinase I: implications for a comprehensive thermostabilization strategy, Biotechnol. Bioeng. 108 (2011) 1841-1851. https://doi.org/10.1002/bit.23144.

[20] Z. Huang, F. Ye, C. Zhang, et al., Rational design of a tripartite fusion protein of heparinase I enables one-step affinity purification and real-time activity detection, J. Biotechnol. 163 (2013) 30-37. https://doi.org/10.1016/j.jbiotec.2012.09.016.

[21] Z. Deng, H. Yang, H. Shin, et al., Structure-based rational design and introduction of arginines on the surface of an alkaline *α*-amylase from *Alkalimonas amylolytica* for improved thermostability, Appl. Microbiol. Biotechnol. 98 (2014) 8937-8945. https://doi.org/10.1007/s00253-014-5790-8.

[22] H. Choi, H.H. Kyeong, J.M. Choi, et al., Rational design of ornithine decarboxylase with high catalytic activity for the production of putrescine, Appl. Microbiol. Biotechnol. 98 (2014) 7483-7490. https://doi.org/10.1007/s00253-014-5669-8.

[23] V. Vasu, J. Kumaresan, M.G. Babu, et al., Active site analysis of *cis*-epoxysuccinate hydrolase from *Nocardia tartaricans* using homology modeling and site-directed mutagenesis, Appl. Microbiol. Biotechnol. 93 (2012) 2377-2386. https://doi.org/10.1007/s00253-011-3548-0.

[24] M.C. Ebert, J.N. Pelletier, Computational tools for enzyme improvement: why everyone can- and should-use them, Curr. Opin. Chem. Biol. 37 (2017) 89-96. https://doi.org/10.1016/j.cbpa.2017.01.021.

[25] N.H.A. Manas, F.D.A. Bakar, R.M. Illias, Computational docking, molecular dynamics simulation and subsite structure analysis of a maltogenic amylase from *Bacillus lehensis* G1 provide insights into substrate and product specificity, J. Mol. Graph. Model. 67 (2016) 1-13. https://doi.org/10.1016/j.jmgm.2016.04.004.

[26] P.J. Hogg, Disulfide bonds as switches for protein function, Trends Biochem. Sci. 28 (2003) 210-214. https://doi.org/10.1016/S0968-0004(03)00057-4.

[27] S. Gleiter, J.C.A. Bardwell, Disulfide bond isomerization in prokaryotes, Biochim. Biophys. Acta. 1783 (2008) 530-534. https://doi.org/10.1016/j.bbamcr.2008.02.009.

[28] D. Fass, Disulfide bonding in protein biophysics, Annu. Rev. Biophys. 41 (2012) 63-79. https://doi.org/10.1146/annurev-biophys-050511-102321.

[29] J.W.H. Wong, S.Y.W. Ho, P.J. Hogg, Disulfide bond acquisition through eukaryotic protein evolution, Mol. Biol. Evol. 28 (2011) 327-334. https://doi.org/10.1093/molbev/msq194.

[30] A.A. Dombkowski, K.Z. Sultana, D.B. Craig, Protein disulfide engineering, FEBS Lett. 588 (2014) 206-212. https://doi.org/10.1016/j.febslet.2013.11.024.

[31] M.M. Bradford, A rapid and sensitive method for the quantitation of microgram quantities of protein utilizing the principle of protein-dye binding, Anal. Biochem. 72 (1976) 248-254. https://doi.org/10.1006/abio.1976.9999.

[32] R.J. Linhardt, A. Grant, C.L. Cooney, et al., Differential anticoagulant activity of heparin fragments prepared using microbial heparinase, J. Biol. Chem. 257 (1982) 7310-7313.

[33] A. Marie, F. Fournier, J.C. Tabet, Characterization of synthetic polymers by MALDI-TOF/MS: investigation into new methods of sample target preparation and consequence on mass spectrum finger print, Anal. Chem. 72 (2000) 5106-5114. https://doi.org/10.1021/ac000124u.

[34] L. Bara, J. Mardiguian, M. Samama, *In vitro* effect on Heptest of low molecular weight heparin fractions and preparations with various anti-IIa and anti-Xa activities, Thromb. Res. 57 (1990) 585-592. https://doi.org/10.1016/0049-3848(90)90075-n.

[35] C. Zhang, B.C. Yang, W.T. Liu, et al., Structure-based engineering of heparinase I with improved specific activity for degrading heparin, BMC Biotechnol. 19 (2019) 59. https://doi.org/10.1186/s12896-019-0553-3.

[36] E. Bramucci, A. Paiardini, F. Bossa, et al., PyMod: sequence similarity searches, multiple sequence-structure alignments, and homology modeling within PyMOL, BMC Bioinformatics. 13(Suppl 4) (2012) S2. https://doi.org/10.1186/1471-2105-13-S4-S2.

[37] V.C. Yang, R.J. Linhardt, H. Bernstein, et al., Purification and characterization of heparinase from *Flavobacterium heparinum*, J. Biol. Chem. 260 (1985) 1849-1857. https://doi.org/10.1016/S0021-9258(18)89671-5.

[38] E. Gray, Standardisation of unfractionated and low-molecular-weight heparin, Heparin-A Century of Progress , 2012, pp. 65-76. https://doi.org/10.1007/978-3-642-23056-1_4.

[39] D.H. Kim, B.T. Kim, S.Y. Park, et al., Degradation of acharan sulfate and heparin by *Bacteroides stercoris* HJ-15, a human intestinal bacterium, Arch. Pharm. Res. 21 (1998) 576-580. https://doi.org/10.1007/BF02975378.

[40] V.G.H. Eijsink, A. Bjørk, S. Gåseidnes, et al., Rational engineering of enzyme stability, J. Biotechnol. 113 (2004) 105-120. https://doi.org/10.1016/j.jbiotec.2004.03.026.

[41] H. Yu, Y. Zhao, C. Guo, et al., The role of proline substitutions within flexible regions on thermostability of luciferase, Biochim. Biophys. Acta BBA-Proteins Proteomics. 1854 (2015) 65-72. https://doi.org/10.1016/j.bbapap.2014.10.017.

[42] H.F. Son, I.J. Cho, S. Joo, et al., Rational protein engineering of thermo-stable PETase from *Ideonella sakaiensis* for highly efficient PET degradation, ACS Catal. 9 (2019) 3519-3526. https://doi.org/10.1021/acscatal.9b00568.

[43] Y. Liu, Z. Liu, Z. Guo, et al., Enhancement of the degradation capacity of IsPETase for PET plastic degradation by protein engineering, Sci. Total Environ. 834 (2022) 154947. https://doi.org/10.1016/j.scitotenv.2022.154947.

[44] Y. Luo, X. Huang, W.L. McKeehan, High yield, purity and activity of soluble recombinant *Bacteroides thetaiotaomicron* GST-heparinase I from *Escherichia coli*, Arch. Biochem. Biophys. 460 (2007) 17-24. https://doi.org/10.1016/j.abb.2007.01.029.

[45] P. Yu, T. Jia, Y. Chen, et al., Improving the activity of heparinase I by the directed evolution, its enzymatic properties and optimal conditions for heparin degrading by recombinant cells, Biochem. Eng. J. 114 (2016) 237-243. https://doi.org/10.1016/j.bej.2016.07.011.

[46] A. Banerjee, A. Saha, B. K. Saha, Understanding the behavior of π-π Interactions in crystal structures in light of geometry corrected statistical analysis: similarities and differences with the theoretical models, Cryst. Growth Des. 19 (2019) 2245-2252. https://doi.org/10.1021/acs.cgd.8b01857.

[47] M.O. Sinnokrot, C.D. Sherrill, High-Accuracy quantum mechanical studies of π−π interactions in benzene dimers, J. Phys. Chem. A. 110 (2006) 10656-10668. https://doi.org/10.1021/jp0610416.

[48] W.J. Wedemeyer, E. Welker, M. Narayan, et al., Disulfide bonds and protein folding, Biochemistry 39 (2000) 7032-7032. https://doi.org/10.1021/bi005111p.

[49] T. Liu, Y. Wang, X. Luo, et al., Enhancing protein stability with extended disulfide bonds, Proc. Natl. Acad. Sci. 113 (2016) 5910-5915. https://doi.org/10.1073/pnas.1605363113.